Journal of Pharmaceutical and Biomedical Analysis 151 (2018) 106–115

Contents lists available at ScienceDirect

Journal of Pharmaceutical and Biomedical Analysis

journal homepage: www.elsevier.com/locate/jpba

Inhibition of UDP-glucose dehydrogenase by 6-thiopurine and its oxidative metabolites: Possible mechanism for its interaction within the bilirubin excretion pathway and 6TP associated liver toxicity

Chamitha J. Weeramange[a], Cassie M. Binns[b], Chixiang Chen[c], Ryan J. Rafferty[a,*]

[a] Department of Chemistry, Kansas State University, 1212 Mid-Campus Drive North, 203 CBC Building, Manhattan, KS 66506, United States
[b] Department of Biochemistry, Kansas State University, 1711 Claflin Road, Manhattan, KS 66506, United States
[c] Department of Statistics, Kansas State University, 101 Dickens Hall, Manhattan, KS 66506, United States

ARTICLE INFO

Article history:
Received 5 October 2017
Received in revised form
24 December 2017
Accepted 29 December 2017
Available online 30 December 2017

Keywords:
6-Thiopurine
UDP-glucuronic acid
Glucuronidation
Drug metabolism
Jaundice

ABSTRACT

6-Thiopurine (6TP) is an actively prescribed drug in the treatment of various diseases ranging from Crohn's disease and other inflammatory diseases to acute lymphocytic leukemia and non-Hodgkin's leukemia. While 6TP has beneficial therapeutic uses, severe toxicities are also reported with its use, such as jaundice and liver toxicity. While numerous investigations into the mode in which toxicity originates has been undertaken. None have investigated the effects of inhibition towards UDP-Glucose Dehydrogenase (UDPGDH), an oxidative enzyme responsible for UDP-glucuronic acid (UDPGA) formation or UDP-Glucuronosyl transferase (UGT1A1), which is responsible for the conjugation of bilirubin with UDPGA for excretion. Failure to excrete bilirubin leads to jaundice and liver toxicity. We proposed that either 6TP or its primary oxidative excretion metabolites inhibit one or both of these enzymes, resulting in the observed toxicity from 6TP administration. Inhibition analysis of these purines revealed that 6-thiopurine has weak to no inhibition towards UDPGDH with a K_i of 288 μM with regard to varying UDP-glucose, but 6-thiouric (primary end metabolite, fully oxidized at carbon 2 and 8, and highly retained by the body) has a near six-fold increased inhibition towards UDPGDH with a K_i of 7 μM. Inhibition was also observed by 6-thioxanthine (oxidized at carbon 2) and 8-OH-6TP with K_i values of 54 and 14 μM, respectively. Neither 6-thiopurine or its excretion metabolites were shown to inhibit UGT1A1. Our results show that the C2 and C8 positions of 6TP are pivotal in said inhibition towards UDPGDH and have no effect upon UGT1A1, and that blocking C8 could lead to new analogs with reduced, if not eliminated jaundice and liver toxicities.

1. Introduction

Acute lymphocytic leukemia (ALL) and non-Hodgkin's leukemia represent two of the more than ten types of leukemia's currently affecting humans [1]. Together, these two forms comprise the nearly 80,000 new cases in 2016, with an approximate death rate of 22,000 in the United States. While current treatments have helped decrease this death rate compared to years past, the estimated 22,000 deaths still represent a large population of people seeking new treatments to help push them into remission. Multiple drugs are currently being employed in the treatment against these leukemias; such as, but not limited to: vincristine (oncovin), cytarabine (Cytosar), doxorubicin (adriamycin), etoposide (VP-16), teniposide (Vumon), methotrexate, cyclophosphamide (Cytoxan), and 6-thiopurine [2–9]. Unfortunately, each of these treatments have failed to decreased the projected 22,000 deaths, mostly due to fatal toxicity associated with the treatments or discontinuation of treatments. 6-Thiopurine (6TP, aka 6-mercaptopurine) has a proven record in the remission of both types of leukemia mentioned previously, but also has a well-documented toxicity associated with its use [9,10]. Through investigations into its mode of toxicity, it is envisioned that new classes/analogs that retain the potent therapeutic character of 6TP, but with greatly diminished if not eliminated toxicity, can be synthesized.

* Corresponding author at: Kansas State University, Department of Chemistry, 1212 Mid-Campus Drive North, Manhattan, KS, United States.
E-mail address: rjraff@ksu.edu (R.J. Rafferty).

https://doi.org/10.1016/j.jpba.2017.12.058
0731-7085/

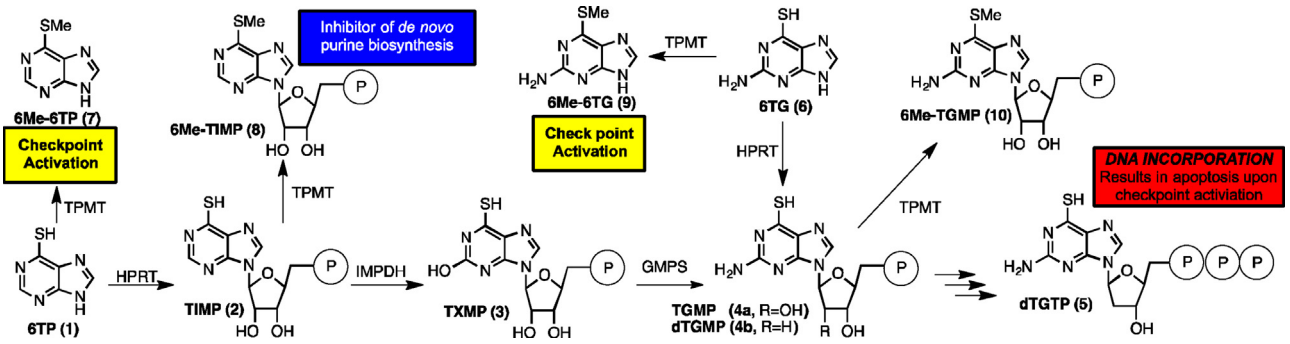

Fig. 1. Anabolic (therapeutic) metabolism of 6-thiopurine (**1**) and 6-thioguanine (**6**) into the dTGTP, a mimic of dGTP for DNA incorporation that results in cell death from base-pair mismatch. Various side metabolic routes of 6TP are presented: i) methylation forming 6-Me-6TP (**7**) and 6Me-6TG (**9**) that induces checkpoint activation triggering cell death from the dTGTP incorporation, and ii) methylation of TIMP (**2**) forming 6-MeTIMP (**8**) that inhibits *de novo* purine biosynthesis.

The therapeutic activity of 6TP (**1**) comes from two main routes: methylation of the thiol of 6TP (**7**) and formation of a deoxythioguanosine triphosphate mimic (dTGTP, **5**) illustrated in Fig. 1. The former metabolite is formed through the methylation of the thiol by thiopurine methyltransferase (TPMT), and has no direct therapeutic activity [11]. The latter is formed through a cascade starting with the phosphoribosylation of 6TP (**1**) by hypoxanthine-guanine phosphoribosyltransferase (HPRT) to access thioinosinic acid (TIMP, **2**). Two key-fates diverge from TIMP, both leading to the therapeutic efficacy [10,12]. En route to its primary therapeutic pathway, **2** is converted to thioxanthine monophosphate (**3**) by inosine monophosphate dehydrogenase (IMPDH). This is normally the rate-limiting step of the pathway, but it has been found that the activity of IMPDH is higher in malignant lymphoblasts and myeloblasts compared to normal lymphocytes [13]. Interestingly, 6TP has been shown to cause an induction of IMPDH which results in a four-fold increase of DNA incorporation of the deoxythioguanine mimic (**5**, *vide infra*). Formation of the thioguanine monophosphate nucleoside (**4a**) is accomplished by guanosine monophosphate synthetase (GMPS). This step also allows for the formation of the deoxyribose (**4b**) [10,12]. Kinase steps convert both **4a** and **4b** into their corresponding triphosphate forms of RNA and DNA (**5**), respectively. Cell death via 6TP administration occurs through the incorporation of the nucleotide **5**, which mimics and competes with endogenous guanosine nucleotides, into DNA. The incorporation of **5** into DNA results in base-pair mismatching and the cell undergoing apoptosis. However, cell death via this mechanism is not immediate [14]. Multiple passages of the S-phase are required to allow for sufficient dTGTP's to be incorporated into DNA; upon checkpoint activation, recognition of the mismatch base pairing is revealed [9,15]. Enhanced checkpoint activation with 6TP-adminstration comes from the methylated thiol species **7** and **9**, formed from the methylation of 6TP (**1**) and 6-thioguine (**6**, 6TG), respectively. Both methylated species have no cytotoxic properties themselves, but both induce checkpoint activation allowing for the identification of mismatching DNA sequences resulting in apoptosis [9]. In addition to methylation forming checkpoint activating species, the methylation of **2** by TPMT forms 6Me-TIMP (**8**), which has been proven to inhibit *de novo* purine biosynthesis [9,16]. Through this inhibition an increased cellular uptake of purines follows, which include 6TP. The increased influx of 6TP allows for increased DNA incorporation of **5** that increases the rate in which apoptosis occurs.

In conjunction to its therapeutic metabolism, there are also detoxification pathways operating simultaneously that greatly reduce the bioavailability of 6TP, shown in Fig. 2. En route to dTGTP (**5**), dTGMP (**4b**) can be used as a substrate for nucleotidases and nucleosidases that results in the formation of 6TG (**6**), which can further be converted to 6-thioxathine (**11**) by guanase. Xanthine oxidase (XO) then oxidizes the C8 position to form 6-thiouric acid (6TU, **12**), which is the terminal excretion metabolite of 6TP [17]. The formation of 6TU can be accomplished directly from 6TP through oxidation by XO, a species that is retained by the body well beyond 24-h post 6TP treatment [14]. It is through this pathway that an excess of 6TP can be redirected, thus preventing formation of 6Me-TIMP and dTGTP for therapeutic activity. Suppression in the formation of 6TU can be accomplished through a combination therapy with XO inhibitors, such as allopurinol [18]. However, said combination results in new and greater toxicity that requires a lower dosage of 6TP. Keeping in mind that high concentrations of dTGTP are required to cause cell death, the resulting 6TP decrease with the allopurinol co-treatment allows for cells to be rescued from this mode of cell death [18]. Likewise, the decreased administration of 6TP also directly reduces the *de novo* purine biosynthesis inhibition caused by 6Me-TIMP, further diminishing its therapeutic efficacy. As such, the combination therapy of XO inhibitors with 6TP fails to produce a beneficial treatment strategy.

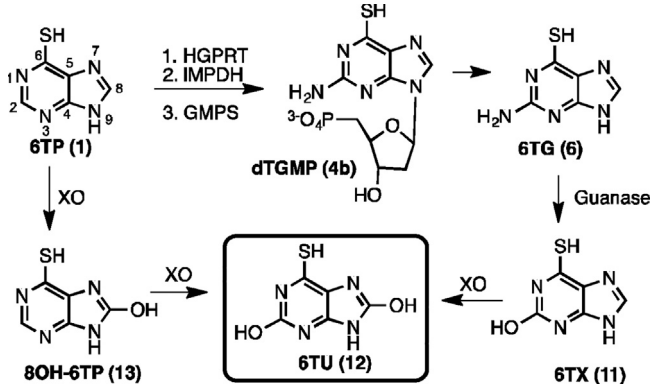

Fig. 2. Formation of 6-thiouric acid (**12**) through two pathways: from degradation of one of the intermediates of the therapeutic pathway (**4b**) and direct oxidation from 6TP by xanthine oxidase (XO).

One of the key toxic side effects of 6TP administration is jaundice; approximately 40% of those taking 6TP develop this life threatening side-effect [19]. The average person forms about 250–300 mg of bilirubin formed per day [20]. Failure to excrete bilirubin can cause jaundice, hyperbilirubinemia, kernicterus, Crigler-Najjar syndrome, Gilbert's syndrome and even death [21–23]. Jaundice results from the buildup of bilirubin within the body, most commonly from the failed detoxification of heme groups (**13**) post red blood cell senescence shown in Fig. 3 [24]. The heme group, comprised of a porphyrin and metal, of the former red blood cell must be degraded and excreted upon senescence of the erythrocyte, commonly referred to as the bilirubin pathway

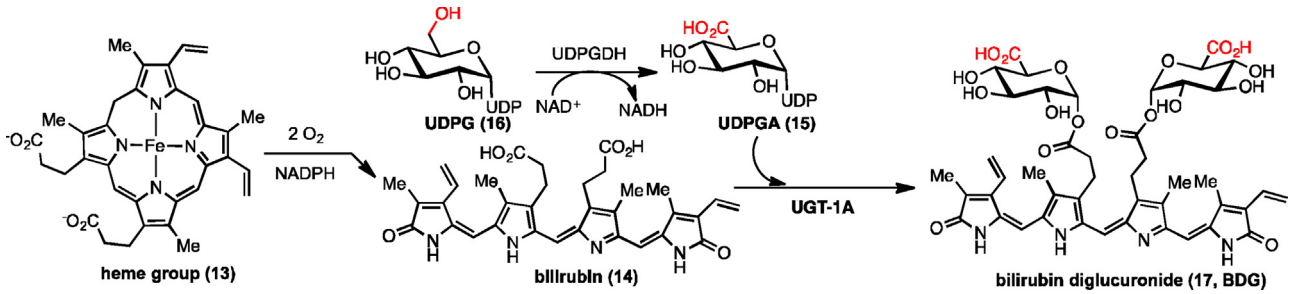

Fig. 3. Formation of the excretable bilirubin diglucuronide species from the conjugation of bilirubin with two UDPGA units.

(Fig. 3) [25]. The bilirubin (**14**) formed is a relatively large, non-polar molecule, whose characteristics make its excretion difficult but critical to prevent jaundice onset as well as liver toxicity. Excretion occurs with the direct conjugation with two UDP-glucuronic acids (**15**, UDPGA) via UDP-glucuronyl transferase (UGT-1A1) [26]. The UDPGA are formed from the oxidation of UDP-glucose (**16**, UDPG) by UDP-glucose dehydrogenase (UDPGDH) [27]. The resulting bilirubin diglucuronide (**17,** BDG) is more water-soluble and thus more easily excreted. The transferase enzyme responsible for this conjugation is located on the smooth and rough endoplasmic reticulum of the liver [28].

We postulate that it is through the inhibition UDPGDH and/or UGT1A1 that causes the severe reported toxicity from 6TP administration, namely jaundice. Furthermore, it is hypothesized that inhibition of one or both of these enzymatic steps is instigated by 6TP and its known excretion metabolites (**11, 12,** and **13**). This study outlines the work into investigating the possible route of toxicity resulting from 6TP administration about these two key enzymatic transformations.

2. Materials and methods

2.1. Chemicals and reagents

All standard chemicals used in this study were the highest grades available and were purchased through Sigma-Aldrich (Saint Louis, MO, USA), VWR (Radnor, PA, USA), or Fisher Scientific (Denver, CO, USA). Specialized reagents were purchased through specific vendors. Glycylglycine (gly-gly: G1127), ß-nicotinamide adenine dinucleotide (NAD^+: N1636), uridine 5′-diphosphoglucose (UDPG disodium salt: U4625), uridine 5′-diphosophoglucuronic acid (UDPGA: U6751), uridine 5′-diphosphoglucose dehydrogenases (UDPGDH: U6885), 6-thiopurine monohydrate (6TP), 6-thioguanine (6TG, A4882), 6-thioxanthine (6TX, T8125), bilirubin (including three mixed isomers, B4126), 4,5-diamino-6-hydroxypyrimidine hemisulfate salt (D19303), alamethicin (A5361), and pooled rat liver microsomes (M9066) were purchased from Sigma-Aldrich. 6-Mercaptopurine-2-ol (6-TX, QA-6668) was purchased from Combi-Blocks, and 6-thiouric acid (6-TU, SC-213040) from Santa Cruz Biotechnology. HPLC-grade water was obtained by passing distilled water through a reverse osmosis system followed by treatment with a Thermo Scientific Barnstead Smart2Pure 3UV purification system (Fisher, 10-451-045), herein referred to as nanopure water.

2.2. Equipment, supplies, data software, and statistical analysis

All standard consumable supplies used in this study were purchased from VWR or Fisher Scientific. Specific equipment utilized in this work are: 1) Hewlett-Packard 8452 Diode Array UV/Vis spectrophotometer (Palo Alto, CA, USA) equipped with a Lauda Brinkman Ecoline RE 106 E100 circulating water bath purchased from VWR, 2) HPLC system consisting of an CBM-20A/20Alite system controller, SIL-20AHT Auto sampler, SPD-20A, SPD-20AV UV–vis Detector, LC-20AT Solvent delivery module, CTO-20A Column Oven, DGU-20A3R Degassing unit and LC-20AD/20AT Gradient Valve Kit purchased from Shimadzu Scientific Instruments (Kyoto, Japan), and 3) all incubated reactions were performed with a Labcare America PRECISION water bath model 25 purchased from Fisher Scientific. All HPLC separations were performed on a Discovery C18 analytical column, 4.6 mm × 100 mm, 5 μm particle size (504955-30) along with the respective guard column (59576) purchased from Sigma-Aldrich. Data was processed and all figures and tables constructed via the program Prism 7.02 for Mac, GraphPad Software (La Jolla, CA, USA). All chemical structures were prepared with ChemDraw Professional 16.0 by PerkinElmer (Waltham, MA). All statistical calculations within this body of work was performed by the treatment of two-ay factorials (positive and negative controls, design structure of RCBD, and T-tests) with Statistical Analysis System (SAS) software for Windows (Cary, NC, USA).

2.3. UDP-glucose dehydrogenase activity assay

Standard preparation: A 0.50 M Gly–Gly buffer (pH 8.7 at 25 °C) was prepared by dissolving 1.62 g of Gly–Gly in 22 mL nanopure water, pH adjusted to 8.7 with 9 M potassium hydroxide and then diluted to 25 mL with nanopure water all while being shaken at 25 °C. Solutions of UDPG and NAD^+ were prepared by dissolving 1.7 mg and 4.5 mg, respectively, into nanopure water resulting in 2 mM and 10 mM solutions, respectively. Preparation of the 0.1 mM 6TU solution was done by dissolving 1.8 mg into 95.5 mL of nanopure water, pH was adjusted to 9.5 with a 2 M sodium hydroxide solution (for solubility), pH adjusted to 7.5 with a 0.5 M hydrochloric acid solution (a dilute solution of HCl is required to prevent thiol oxidation), and then diluted to 100 mL. In an analogous fashion, samples of 6TP, 6TX, and 8Me-6TP were prepared. A 5 unit/mL UDPGDH solution was prepared by dissolving 0.11 mg of UDPGDH in 0.8 mL of 0.5 M Gly–Gly while stirring; once dissolved, the solution was diluted to volume with gly–gly in a 1 mL volumetric flask. All solutions were kept at 4 °C when not in use.

2.3.1. Inhibitor assessment – general procedure

Spectrometric analysis was performed on a Hewlett-Packard 8452 Diode Array UV/Vis spectrometer equipped with a Lauda Brinkman Ecocline RE 106 E100 circulating water bath. The water bath was maintained at 25 °C and the diode array was set at 340 nm, both were allowed to warm up 10-min prior to analysis. To a 1 mL cuvette, 300 mL of 0.5 M Gly–Gly (0.15 M final concentration), nanopure water, varying NAD^+ and UDPG concentration in varying inhibitor concentrations were added and placed in the diode array for a 2 min thermal equilibration. Once 1.5 min elapsed, the instrument was zeroed to obtain an initial rate change in absorbance versus time. The reaction was initiated by addition of 20 μL of the UDPGDH solution. Thorough mixing by inversion of the cuvette was

performed as quickly as possible and then placed in the holder for analysis. The reaction was monitored from 20 to 120 s after enzyme addition, and the slope was calculated from 20 to 40 s using the diode array software.

Inhibitor Assessment – Saturating NAD^+ varying UDPG concentration: For each analysis, the cuvette was prepared in the same fashion as outlined above. The final concentration of the components of the mixture were 150 mM Gly-Gly, 0.1 unit/mL UDPGDH, 3 mM NAD^+ and varied concentrations of 0.1, 0.05, 0.025 and 0.02 mM of UDPG, obtained from stock solution addition. Nanopure water was used as a variable component to ensure that a final volume of 1 mL was obtained. Inhibitor analysis of the four purines was performed at two concentrations: 50 and 100 μM for 6TP, 20 and 50 μM for 6TX and 8OH-6TP, and 5 and 10 μM for 6TU, obtained from their corresponding stock solutions. Each assessment was performed in triplicate. The average of the three were plotted and the slopes were used to determined inhibition values.

Inhibitor Assessment – Saturating UDPG varying NAD+ concentration: In an analogous protocol as described for NAD^+ saturating conditions (above), inhibitor analysis of UDPGDH was performed under UDPG saturating conditions (0.6 mM) with varying concentrations of NAD^+.

2.4. UDP-glucuronosyltransferase activity assay

Standard preparation: A bilirubin stock solution was prepared by dissolving bilirubin in 100% dimethyl sulfoxide to yield a concentration of 2 mM, the stock solution was aliquoted, and stored at −70 °C until use. A 25 mM UDPGA stock solution was prepared by diluting 8 mg to 0.5 mL with nanopure water, and a 10 mg/mL alamethicin solution was prepared by taking 5 mg and diluting to 500 μL with methanol. Preparation of the 100 mM potassium dihydrogen phosphate buffer was done by dissolving 2.3 g of KH_2PO_4 into 80 mL of nanopure water, pH adjusted to 7.4 with 1 M HCl and diluted to volume in a 100-mL volumetric flask.

2.4.1. Chromatographic conditions – bilirubin and bilirubin glucuronide

Bilirubin and its glucuronide were separated on a Discovery C18 analytical column, 4.5 mm x 100 mm, 5 μM particle size with guard column. A dual mobile phase was employed; the aqueous phase consisted of an 8 mM imidazole & 2.5 mM tetrabutylammonium hydrogen sulfate (TBAHS) buffer at a pH of 6.5 in nanopure water and acetonitrile as the organic phase. A gradient elution profile was employed for full separation at a flow rate of 0.5 mL/min, the method begins at 10% acetonitrile and increases to 50% over 8 min, held for 5.5 min, increased to 95% over 4.5 min, held for 10 min, returned to 10% over 4 min and held at 10% for 2 min to allow for column regeneration. The detection wavelength was 450 nm with a sample injection volume of 5 μL. The combined peak area for bilirubin (sum of the three isomers) was plotted relative to the concentration prepared for the generation of a working standard curve.

Chromatographic Conditions – UDPGA: Chromatographic separations were performed on a Discovery C18 analytical column, 4.5 mm × 100 mm, 5 μm particle size (Supelco) with a guard column. UDPGA was separated under isocratic conditions, flow rate at 0.5 mL/min using a mobile phase comprised of 40% methanol and 60% buffer that was composed of 8 mM imidazole and 5 mM TBAHS at a pH of 6.5. The detection wavelength was 262 nm with a sample injection volume of 5 μL. Various concentrations of UDGPA were analyzed, and peak areas obtained were plotted relative to said concentrations to generate a working standard curve.

Quantification of Bilirubin, Mono/Di-glucuronide, and UDPGA Levels: Standard curves for both bilirubin and UDPGA were constructed and used for the quantification of each species. Bilirubin was quantified directly from the generated standard curve. A total of ten peaks for the glucuronide species, including their isomers were detected in the incubation samples. Peak assignment and identification of UCB, BMG1, BMG2, BDG and their isomers were based on their lipophilicity and polarity, as well as the elution pattern, chromatographic peak position and relative retention time from previous reports [21–23]. The calibration curves for bilirubin were used to determine the concentration of the mono- and di-glucuronide species employing the gradient HPLC bilirubin method described above. Quantification of UDPGA levels was determined through the use of the constructed standard curve within the isocratic HPLC method developed for UDGPA.

Bilirubin Glucuronide Formation: Bilirubin glucuronidation was performed at 37 °C in a shaking water bath. All steps taken were performed in the lowest light conditions possible; the glucuronide formed was found to be unstable to ambient lighting. The following was added to an Eppendorf tube to achieve the final concentrations indicated, final volume 200 μL: potassium phosphate buffer (50 mM, pH 7.4), bilirubin (10 μM), $MgCl_2{\cdot}6H_2O$ (0.88 mM), rat liver microsomes (RLM, 100 μg of protein/mL), alamethicin (22 μg/mL), and allowed to pre-incubated for 2 min. Addition of UDPGA (3.5 mM), referred to as the zero-time point, initiated the reaction. The mixture was allowed to shake at 37 °C for each of the time course experiments. To each reaction 600 μL of ice-cold methanol containing 200 mM ascorbic acid was added to terminate the enzymatic reaction, vortexed for 2 min, and then centrifuged at 12,000 rpm for 10 min. The supernatant was then analyzed by the developed gradient HPLC protocol for separation and quantification of UCB, BMG1, BMG2, and BDGs.

Validation of Bilirubin Glucuronide Formation: Quantification of UCB, BMG1&2 and BDGs were performed post the quenching of UGT1A1, which was performed by immersing the Eppendorf tube with the reaction mixture in a cold-water bath for two min. No ascorbic acid was used, as the residual material would quench the glucuronidase enzyme to be added. To this sample 0.1 mg/mL glucuronidase enzyme was added, inverted (x3), and then analyzed by the HPLC protocol developed to quantify the levels of bilirubin and BMG1&2 and BDGs for formation confirmation.

Inhibitor Assessment of Bilirubin Glucuronide Formation: Employing the same protocol delineated above for the formation of the bilirubin glucuronide species, inhibitor assessment was performed. To the Eppendorf tube, 6-thiopurine or 6-thiouric acid (50 and 75 μM final concentrations) was added alongside a control (no purine added) and allowed to pre-incubate for 2 min. Addition of UDPGA initiated the reaction for each of the time course experiments. The gradient HPLC method was employed for the 45-min time course experiments for the quantification of the glucuronide species. For experiments in which UDPGA was analyzed, the incubation protocol for the formation was altered as follows: 300 μL final volume, 2.5 μM of bilirubin, 260 μM of UDPGA was employed to start the reaction, no alamethicin, and the enzyme was quenched with heat (87 °C). Quantification of UDPGA for the 1, 12, and 15-h time course experiments was performed by the isocratic HPLC method described above.

2.5. Synthesis of 8-OH-6-Thiopurine

From commercially available 4,5-diamino-6-hydroxypyrimidine, thiol installation about the C6 position was accomplished under standard employed protocols with Lawesson's reagent [29] in a 43% yield. Following a Traube synthesis protocol [30], 4,5-diamino-6-thiopyrimidine was heated with urea in muffle furnace until the mixture underwent a molting process. The reaction was worked up under acid-base conditions followed by recrystallization to afford the desired 8OH-6-thiopurine in a 65% yield. The product matched reported

characterization data (NMR included within the Supplemental Material).

3. Results and discussion

3.1. Inhibition profiling of UDPGDH by 6TP, 6TU & 6TX

Assessment of activity/inhibition of NAD(P)-dependent dehydrogenase catalyzed reactions is commonly and routinely performed by UV/Vis spectrometry methods by monitoring absorbance changes at 340 nm [31]. The only caveat to performing assessment of activity in this fashion is that any substrate/inhibitors to be screened must not absorb at 340 nm. If wavelength overlap is present, it can make it difficult, or even impossible to determine if there are any substrate/inhibitor effects upon the enzymatic reaction. Purines, such as 6-thiopurine and its main excretion metabolites absorb at 340 nm and therefore prevent assessment of enzymatic activity in commonly employed assays. To overcome the interfering signal, we found that if the purines were screened in sufficiently low concentration, such that the magnitude of their absorbance at 340 nm is relatively non-interfering, that inhibition studies could be performed against UDPGDH in a rapid and reproducible fashion. Through spectral experimentation the following allowable maximum concentrations were found that had negligible interference at 340 nm: 100 μM for 6TP, 50 μM for 6TX, and 10 μM for 6TU. Lower concentrations were then analyzed for generation of inhibition profiles for 6TP, 6TU, and 6TX toward UDPGDH. Inhibition was assessed through saturation kinetics, in which either UDPG or NAD^+ was saturating while the other substrate concentration was variable.

Inhibition profiles for 6TP, 6TU, and 6TX against UDPGDH with varying UDPG and saturating NAD^+ is shown in Fig. 4A–C, and varying NAD^+ with saturating UDPG is presented in Fig. 4D–F. For each purine screened, three separate experiments were performed: no purine, and purine at both low and high concentration levels. From the analysis with no purine, under both varying UDPG and NAD^+ conditions, the K_m and V_{max} were calculated. The determination of the K_i was accomplished by plotting the slope from each independent analysis set versus the concentration of purine; calculation of the K_i was performed by taking the negative-inverse value of the x-intercept. Table insert within Fig. 4 summarizes the respective K_i, K_m, and V_{max} values for each purine in respect to both varying and saturating concentrations of UDPG and NAD^+ concentrations.

3.2. Synthesis of 8-OH-6-thiopurine and UDPGDH inhibition profiling

To assess the full effects of hydroxylation about the C2 and C8 positions (purine numbering shown in Fig. 4 table insert) of 6TP excretion metabolites, the synthesis of 8OH-6TP was undertaken from reported procedures in 28% yield over two-steps (Fig. 5) [30]. In an analogous fashion to the three purines described above, 8OH-6TP was assessed for inhibition towards UDPGDH. Fig. 6 outlines the inhibition of the C8 hydroxylated purine under varying UDPG concentration (Fig. 6A) and varying NAD^+ concentration (Fig. 6B). In regards to both, 8OH-6TP was found to inhibit UDPGDH more potently than 6TX (varying about the position of hydroxylation) and comparably to 6TU. The K_i with respect to varying UDPGA was found to be 14 μM and with respect to varying NAD^+ 32.5 μM.

3.3. Inhibition effects of 6TP and 6TU upon UGT1A1

Further investigation into the bilirubin detoxification pathway led to inhibition studies of 6TP and 6TU towards UGT1A1. Only 6TP and 6TU were screened, as they represented the two extremes of inhibition towards UDPGDH with regards to varying UDPGA concentrations. To assess inhibition, an HPLC method was developed that allowed for the separation and quantification of all substrates and products from the UGT1A1 reaction. While there are reported methods to assess the activity of this transferase reaction [21–23], our method developed includes universal applications of each, as well as new aspects. This method allows for the full separation and quantification for all bilirubin glucuronide species and unconjugated bilirubin, as well as applications into inhibition assessment.

Shown in Fig. 7-line A are the three isomers of unconjugated bilirubin (UCB) from 23.6–24.2 min. Line B the three isomers of the bilirubin diglucuronide (BDG) species at 11.2–11.4 mins and the various bilirubin monoglucuronides (BMG1&2) from 12.3–13.2 mins. To validate the formation of the various glucuronide species, a separate reaction was run and then treated with glucuronidase, which removes the glucuronic acid upon the various forms of the bilirubin glucuronide species forming unconjugated bilirubin and glucuronic acid. Line C is obtained post glucuronidase treatment of the formed glucuronide species from line B. With the results from Fig. 7, the formation of the glucuronide species is thereby confirmed and in extension confirms the validity of the method developed for separation of substrates and products [21].

Standard curves for both the mono- and di-glucuronide species was unattainable, given that both species are both light and thermally sensitive and have been found to degrade rapidly [21,22]. To this end, the bilirubin standard curve was employed given that the same chromophore species is present within UCB, BMG1&2, and BDG. Inhibition assessment of 6TP and 6TU was performed at 50 and 75 μM for both purines over a 45-min incubation period. Outlined in Fig. 8 are the levels of the BDG, the various BMG1&2, and UCB when treated with 50 and 75 μM of 6TP. Inhibition investigations by 6TU at the same conditions are shown in Fig. 9. The apparent values for the formation of BMGs, BDG, and remaining UCB showed no significant difference ($P > 0.05$) in the presence and absence of 6TP and 6TU. All statistical calculations are presented within the Supplementary Material. Stability of the glucuronide species could present doubt in the accuracy of the quantification and in turn the validity of the inhibition profiles obtained. Therefore, assessment of inhibition by indirect means of a stable species could further validate the findings from the glucuronide study.

3.4. 6TP & 6TU inhibition of UGT1A1 via UDPGA quantification

Due to the well reported and documented instability of the glucuronide species, activity of UGT1A1 was assessed by monitoring and quantifying UDPGA levels. The previous HPLC method for glucuronide quantification was not applicable for UDPGA quantification due to the elution of UDPGA at a gradient point in the method. Therefore, an isocratic HPLC assay with UV detection at 262 nm was developed for quantification of UDPGA that allows for the indirect quantification of BMG1&2 and BDG formation. Successful conjugation of bilirubin to either one or two UDPGAs will form the desired glucuronide species, and upon any degradation of these thermally and light reactive species will result in the return of UCB and glucuronic acid. The glucuronic acid will have a different retention factor in comparison to UDPGA. Therefore, any decrease in UDPGA levels directly corresponds to the formation of the glucuronide species. A standard curve for UDPGA was generated to access concentration in this work (presented in the supplemental material). Thermal stability of UDPGA is key for this method, and was determined by incubating UDPGA in the reaction media over a 15-h period (shown in Fig. 10 with comparison between UDPGA and mixture with no enzyme added at 37 °C).

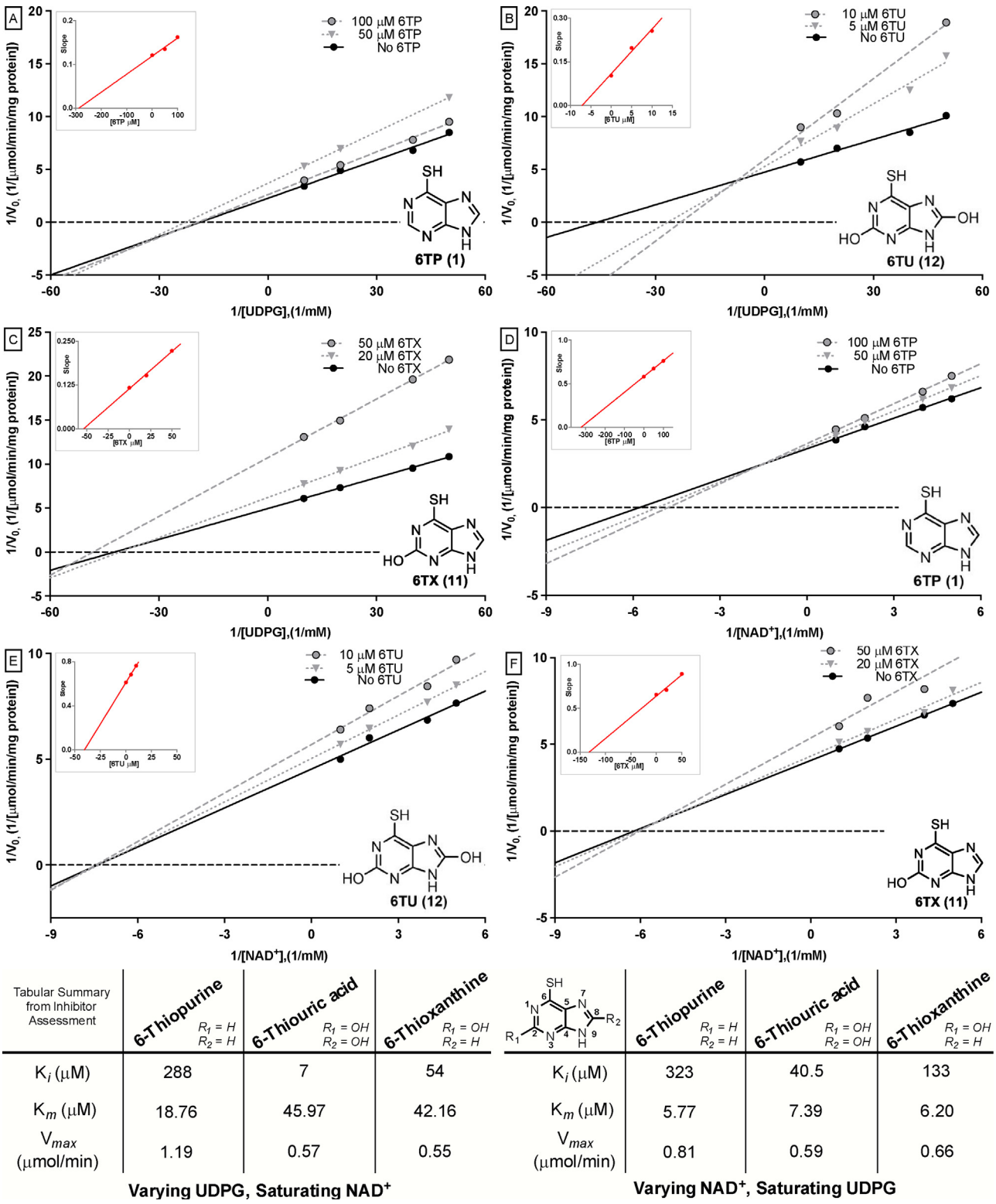

Tabular Summary from Inhibitor Assessment	6-Thiopurine (R_1 = H, R_2 = H)	6-Thiouric acid (R_1 = OH, R_2 = OH)	6-Thioxanthine (R_1 = OH, R_2 = H)
K_i (μM)	288	7	54
K_m (μM)	18.76	45.97	42.16
V_{max} (μmol/min)	1.19	0.57	0.55

Varying UDPG, Saturating NAD^+

	6-Thiopurine (R_1 = H, R_2 = H)	6-Thiouric acid (R_1 = OH, R_2 = OH)	6-Thioxanthine (R_1 = OH, R_2 = H)
K_i (μM)	323	40.5	133
K_m (μM)	5.77	7.39	6.20
V_{max} (μmol/min)	0.81	0.59	0.66

Varying NAD^+, Saturating UDPG

Fig. 4. Inhibition assessment towards UDP-glucose dehydrogenase by various 6TP excretion metabolites through Lineweaver-Burk plot analysis under UDPG varying NAD^+ saturating conditions. A) Concentrations of 6TP, varying UDPG, screened were 0, 50, & 100 μM with slopes of each line 0.121, 0.135, 0.1623 respectively. Plotting slopes versus concentration afforded a regression line of y = 0.000413x + 0.1188. B) Concentrations of 6TU, varying UDPG, screened were 0, 5, & 10 μM with slopes of each line 0.103, 0.198, 0.2565 respectively. Plotting slopes versus concentration afforded a regression line of y = 0.0154x + 0.1091. C) Concentrations of 6TX, varying UDPG, screened were 0, 20, & 50 μM with slopes of each line 0.117, 0.152, 0.223 respectively. Plotting slopes versus concentration afforded a regression line of y = 0.0021x + 0.1143. D) Concentrations of 6TP, varying NAD^+, screened were 0, 50, & 100 μM with slopes of each line 0.580, 0.674, 0.760 respectively. Plotting slopes versus concentration afforded a regression line of y = 0.0018x + 0.5813. E) Concentrations of 6TU, varying NAD^+, screened were 0, 5, & 10 μM with slopes of each line 0.614, 0.685, 0.765 respectively. Plotting slopes versus concentration afforded a regression line of y = 0.0154x + 1091. F) Concentrations of 6TX, varying NAD^+, screened were 0, 20, & 80 μM with slopes of each line 0.655, 0.708, 0.891 respectively. Plotting slopes versus concentration afforded a regression line of y = 0.0048x + 6387.

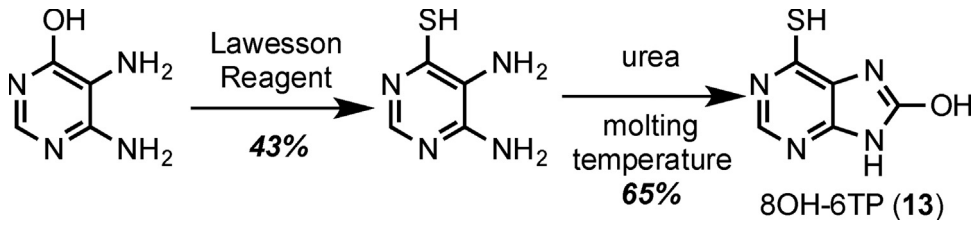

Fig. 5. Synthesis of 8OH-6TP via a modified Traube approach. Thiol installation through Lawesson reagent upon commercially available 4,5-diamino-6-hydroxylpyrimidine with subsequent purine formation via condensation with urea.

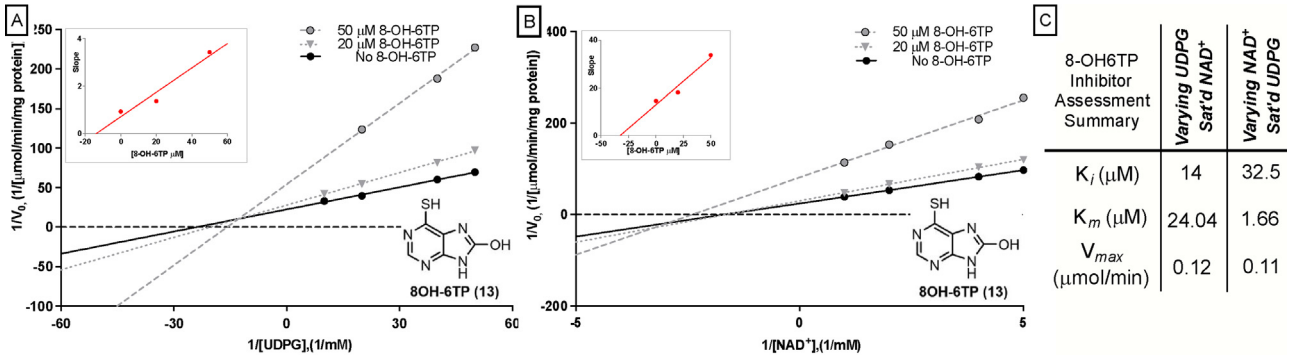

Fig. 6. Lineweaver-Burk inhibitor assessment of 8OH-6TP under varying UDPG saturating NAD^+ conditions (left), varying NAD^+ saturating UDPG (center), and inhibitor summary (right). Concentrations of 8OH-6TP screened were 0, 20, & 50 μM under both condition with slopes of each line for varying UDPG 0.9365, 1.368, 3.422, respectively, and varying NAD^+ 14.54, 18.12, 33.81, respectively. Plotting slopes versus concentration afforded a regression line of y = 0.0512x + 0.7142 for varying UDPG and y = 0.3963x + 12.91 for NAD^+.

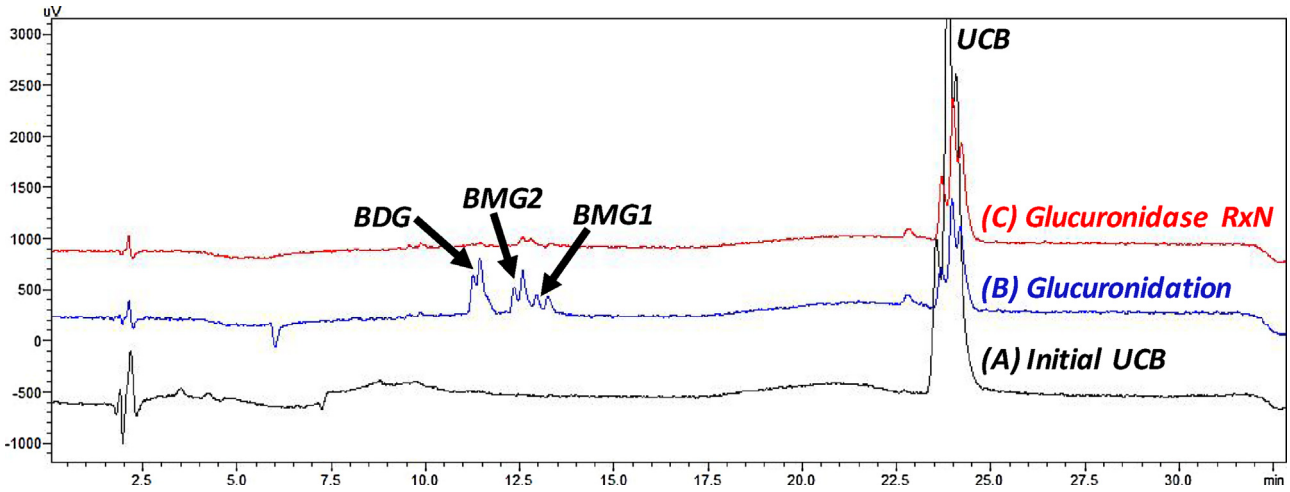

Fig. 7. Chromatograms showing the standard unconjugated bilirubin (line A), formation of the glucuronide bilirubin species (line B), and the UCB obtained post glucuronidase treatment of a sample containing BMG1&2 and BDG for validation of glucuronide formation. The gradient HPLC method was employed with a detection of 450 nm.

Three time-course experiments were performed (1, 12 & 15-h) in which UDPGA concentrations were determined by HPLC analysis (Fig. 10). When the reaction was performed in the absence of any inhibitors, concentrations of UDPGA dropped to 241 μM after 1-h, 110 μM after 12-h, and 17 μM after 15-h from the initial 260 μM (validated by aliquot removal prior to the start of the reaction). Levels of UDPGA were found to be relatively the same when testing inhibition by 50 and 75 μM of 6TP: 241 & 242 for 1 h, 130 & 128 for 12 h, and 20 & 20 for 15 h, respectively. Inhibitor assessment of 6TU towards UGT1A1 afforded similar results to 6TP and the control when screened at 50 and 75 μM of 6TU: 243 & 241 for 1 h, 128 & 125 for 12 h, and 20 & 16 for 15 h, respectively. The apparent UDPGA levels at the end of the reaction showed no significance difference ($P > 0.05$) in the presence and absence of 6TP and TU. All statistical calculations are presented within the Supplementary Material.

4. Conclusion

In the study presented, we have investigated the possible correlations between the excretion metabolites (6TX, 8-OH-6TP, and 6TU) associated with 6TP and the severe toxicities resulting from its administration. These side-effects are so potent that as a result, the

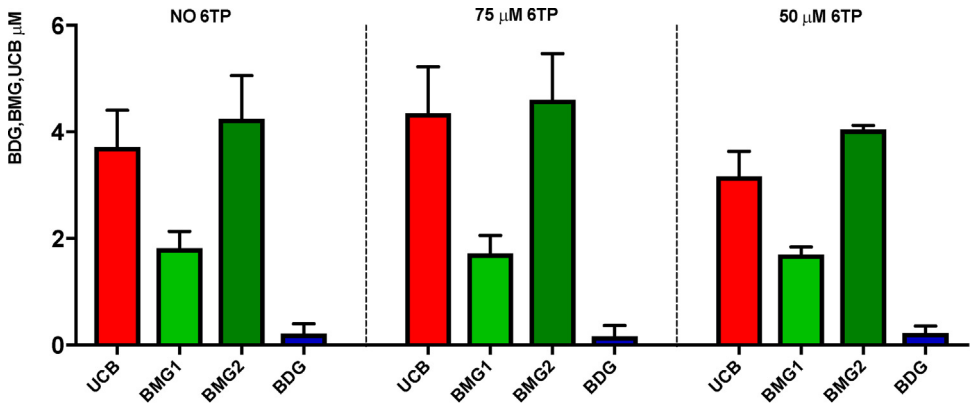

Fig. 8. Inhibition studies of UDP-glucuronosyl transferase (UGT1A1) by 6TP at 50 and 75 μM. Levels of unconjugated bilirubin (UCB), monoglucuronide bilirubin (BMG1 & BMG2), and diglucuronide bilirubin (BDG) quantified through the bilirubin standard curve (presented in the supplemental material). Each analyte is an average of three independent runs with standard error bars.

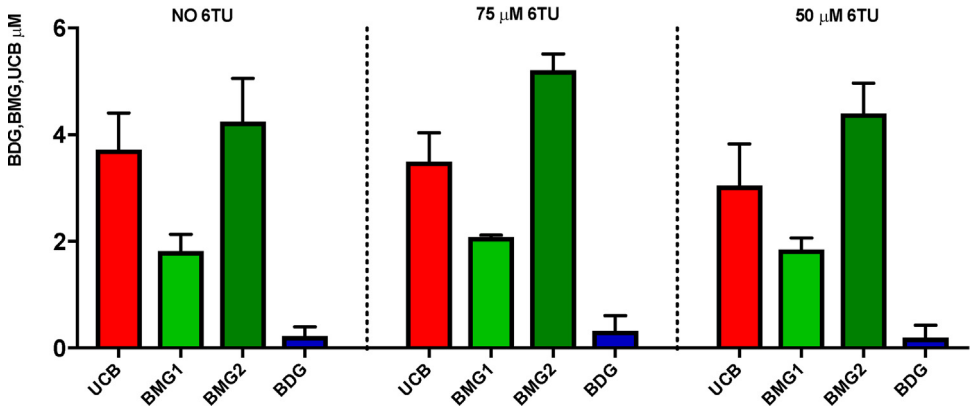

Fig. 9. Inhibition studies of UDP-glucuronosyl transferase (UGT1A1) by 6TU at 50 and 75 μM. Levels of unconjugated bilirubin (UCB), monoglucuronide bilirubin (BMG1 & BMG2), and diglucuronide bilirubin (BDG) quantified through the bilirubin standard curve (presented in the supplemental material). Each analyte is an average of three independent runs with standard error bars.

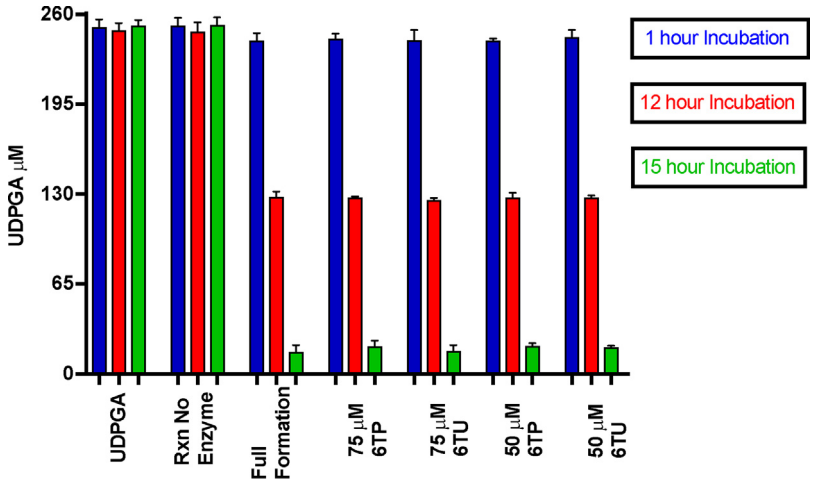

Fig. 10. Assessment of UGT1A1 inhibition by 6TP and 6TU at 75 and 50 μM over three time-course experiments of 1, 12 and 15-h. One-hour incubations are triplicates of triplicates, 12-h are triplicates, and 15-h are triplicates of duplicates.

administration of the drug is given in an on/off strategy allowing time for said toxic species to be cleared by the body. Unfortunately, this greatly reduces the therapeutic efficacy. Severe liver damage is commonly associated with 6TP administration, and given the degree of red blood senescence within leukemia, it is proposed that liver toxicity results from the failed clearance of bilirubin. The two key reactions responsible for bilirubin excretion are: 1) UDPGA formation from UDPG via UDP-glucose dehydrogenase (UDPGDH), and 2) bilirubin conjugation with UDPGA forming the excretable species via UDP-glucuronosyl transferase. As described above, in addition to the therapeutic pathway for 6TP, there is an excretion pathway operating concurrently and at a faster rate. These excretion metabolites are proposed to be responsible for the associated toxicity, specifically through inhibition of UDPGDH and/or UGT1A1.

Table 1
Inhibition assessment of UGT1A1 with regards to varying 6TP and 6TU concentrations. Each data set was run in triplicate with standard deviation values given in parentheticals.

Bilirubin Species	Control	50 μM 6TP	75 μM 6TP	50 μM 6TU	75 μM 6TU
UCB	3.72 μM (±0.38)	3.17 μM (±0.46)	4.35 μM (±0.87)	3.05 μM (±0.77)	3.49 μM (±0.54)
BMG1	1.82 μM (±0.04)	1.70 μM (±0.14)	1.72 μM (±0.34)	1.85 μM (±0.21)	2.09 μM (±0.03)
BMG2	4.24 μM (±0.34)	4.05 μM (±0.07)	4.61 μM (±0.86)	4.40 μM (±0.56)	5.21 μM (±0.30)
BDG	0.23 μM (±0.02)	0.23 μM (±0.13)	0.17 μM (±0.19)	0.19 μM (±0.23)	0.32 μM (±0.28)

Inhibition of UDPGDH by 6TP, 6TX, and 6TU was performed via a new UV/Vis method that was developed. The K_i values were determined for both UDPG and NAD^+ under varying concentrations; given the endogenous concentrations of NAD^+, only the varying UDPG K_i values are discussed. It is of note that the K_i values found upon varying NAD^+ conditions followed the same pattern as those of varying UDPG. The K_i values from these three purines revealed a fascinating pattern of hydroxylation and corresponding inhibition properties. It was found that 6-thiopurine possessed low inhibition character towards UDPGDH with a K_i of 288 μM. Interestingly, it was observed that 6-thiouric acid, the terminal excretion metabolite, possessed the greatest inhibition towards UDPGDH with a K_i of 7 μM in comparison to 288 μM for 6TP. This data set suggests that hydroxylation about the C2 and C8 positions might be pivotal in the inhibition of UDPGDH. Strikingly, when C2 is hydroxylated, inhibition is reduced by three-fold as observed with 6-thioxanthine.

To reveal the entire picture of hydroxylation effects about C2 and C8 with regards to UDPGDH inhibition, the assessment of 8OH-6TP was performed. While this compound is commercially available, its cost is academically prohibitive, and therefore a synthetic route was established. With a synthetic route in place, inhibition towards UDPGDH was performed, and it was found to have a K_i of 14 μM relative to varying UDPG concentration. Correlating the K_i values of the four excretion metabolites to the hydroxylation patterns suggests that the C8 hydroxyl has a greater inhibition character than C2 towards UDPGDH.

Inhibition assessment of these excretion metabolites towards UGT1A1 could not be accomplished through the same UV/Vis method. As such, a method was developed that allowed for baseline separation of all substrates and all glucuronide species. Illustrated in Fig. 7 line B shows the baseline separation of all substrates and products from UGT1A1 at 450 nm. The peaks for each bilirubin species is due to the multiple isomers of bilirubin; 3 for UCB, 2 for BMG1, 2 for BMG2, and 3 for BDG. To confirm that BMG1&2 and BDG are in fact the mono- and di-glucuronide species, a glucuronidase reaction was performed. In this, glucuronide groups are hydrolyzed to afford glucuronic acid and UCB, in this case. As observed in Fig. 7 line C, the glucuronidase experiment upon a pre-formed reaction mixture (Fig. 7 line B) showed the absences of any of the proposed glucuronide species that were previously observed, thereby confirming that the glucuronide formation was successful and that the method is sound. Additional confirmation on the identity of these peaks was drawn from other published methods [31–34].

With a method in place, inhibition screening by the excretion metabolites was undertaken. The bilirubin standard curve generated was found to have a linearity range of 2.5 μM to 8.5 μM. Quantification of bilirubin was accomplished from this standard curve with great accuracy and sensitivity. It is well documented that the glucuronide species formed from bilirubin are light sensitive, and prone to rapid degradation [21–23]. As such, generation of a standard curve of these species can be problematic and thereby prevent proper assessment of activity of UGT1A1 in the presence of our proposed inhibitors. This issue was circumnavigated given that the detectable moiety within these species is the bilirubin core; therefore, quantification of these species could be done through the bilirubin standard curve. Inhibition assessment of UGT1A1 by 6TP and 6TU was performed at two concentrations, but 6TX and 8OH-6TP were not screened, as 6TP and 6TU represent the two extremes of inhibition with regard to UDPGDH. The concentrations of the various bilirubin species were determined after a 45-min period at the varied purine concentration summarized in Table 1. From this, it can be concluded that there is no inhibition of UGT1A1 by either purine at varying concentrations over a 45 min period.

Table 2
Inhibition assessment of UGT1A1 with regards to varying 6TP and 6TU concentrations as quantified by UDPGA consumption. Each data set was run in triplicate with standard deviation values given in parentheticals.

	Duration of the Reaction		
	1-h	12-h	15-h
UDPGA Control	241 μM (±5.6)	110 μM (±0.06)	17 μM (±4.9)
RxN No Enzyme	252 μM (±5.6)	243 μM (±0.07)	253 μM (±5.6)
Full RxN	251 μM (±5.2)	245 μM (±0.21)	252 μM (±4.2)
75 μM 6TP	242 μM (±3.4)	128 μM (±3.08)	20 μM (±3.5)
75 μM 6TU	241 μM (±7.5)	125 μM (±0.05)	16 μM (±4.2)
50 μM 6TP	241 μM (±1.7)	130 μM (±0.05)	20 μM (±2.1)
50 μM 6TU	243 μM (±5.1)	128 μM (±2.16)	20 μM (±0.7)

It is well documented that 6TU remains in the body for more than 24 h post 6TP administration, and as such, one must consider that inhibition of the UGT1A1 occurs well beyond the 45-min experiment described above. Performing the inhibition experiment outlined previously through the quantification of the glucuronide species is not feasible due to the extreme sensitivity of the glucuronide compounds. Therefore, an indirect method to assess inhibition was undertaken through the quantification of UDPGA. Inhibition assessment was performed at the same concentrations of each purine as within the bilirubin assessment, but at varied reaction times of 1, 12, and 15 h. Statistical analysis of all inhibition studies towards UGT1A1 was performed, and it was concluded that all adjusted P-values are larger than 0.05, which indicates that there might be no difference between main effects of treatments and control, thereby verifying that 6TP and 6TU possess no inhibition properties towards UGT1A1 (Table 2).

In summary, we have proposed that the toxic side-effects associated with 6TP administration arises from the inhibition of either or both UDP-glucose dehydrogenase (UDPGDH) or UDP-glucuronosyl transferase (UGT1A1) by 6TP and/or its main excretion metabolites 6TU, 6TG, and/or 6TX. We directed our study towards the clearance of bilirubin, given that liver toxicity is one of the most commonly reported toxicities associated with 6TP administration. As such, the bilirubin pathway was investigated, and no inhibition was observed by both 6TP and 6TU over a 15-h period at concentrations that exceed drug dosing towards UGT1A1. However, inhibition by these purines, as well as the other excretion metabolites towards UDPGDH, was observed. Through these inhibition studies it was discovered that the hydroxylated C2 and C8 positions, namely 6TU, resulted in the greatest inhibition. Said inhibition will directly impact the levels of UDPGA that, in turn, will affect bilirubin conjugation and excretion. While C2 shows inhibition, no alteration at this site is possible as it is directly required for the formation of the nucleotide mimic for DNA incorporation – the primary therapeutic metabolite. The C8 position, on the contrary, can be studied for possible analog construction in the aims of reducing, if not eliminating, the toxicity associated from 6TP administration. Currently

work is being directed in the synthesis of new analogs about the C8 position that hopefully will possess reduced inhibition towards UDPGDH, but retain the therapeutic efficacy of 6-thiopurine.

Funding sources

This work could not have been undertaken without the gracious financial support from the Johnson Cancer Center of Kansas State University and Startup Capital from Kansas State University.

Conflict of interest

The authors declare that they have no conflicts of interest with the contents of the article.

Author contributions

CJW conducted nearly all of the experiments, analyzed the results, and helped write the manuscript. CMB helped with the initial stages of the bilirubin assay development. CC performed all statistical calculations for inhibitory assessment of UGT1A1. RJR conceived the idea for the project, helped with initial training, and wrote the paper; all authors edited and approved the manuscript.

Acknowledgements

We would like to thank Dr. James Mott of Shimadzu Scientific Instruments, Inc. for invaluable discussions on HPLC method development and instrument parameters. We would also like to thank Olivia Haney for technical writing aspects of this manuscript. This paper is dedicated in the memory of Lanny Rafferty.

Appendix A. Supplementary data

Supplementary data associated with this article can be found, in the online version, at https://doi.org/10.1016/j.jpba.2017.12.058.

References

[1] J.M. Torpy, C. Lynm, R.M. Glass, Acute lymphoblastic leukemia, JAMA 301 (4) (2009) 452.
[2] T. Tsuruo, H. Iida, S. Tsukagoshi, Y. Sakurai, Overcoming of vincristine resistance in P388 leukemia in vivo and in vitro through enhanced cytotoxicity of vincristine and vinblastine by verapamil, Cancer Res. 41 (5) (1981) 1967–1972.
[3] P.A.J. Speth, Q.G.C.M. van Hoesel, C. Haanen, Clinical pharmacokinetics of doxorubicin, Clin. Pharmacokinet. 15 (1) (1988) 15–31.
[4] K.R. Hande, Etoposide: four decades of development of a topoisomerase II inhibitor, Eur. J. Cancer 34 (10) (1998) 1514–1521.
[5] N.S. Elbarbary, E.A.R. Ismail, R.K. Farahat, M. El-Hamamsy, ω-3 fatty acids as an adjuvant therapy ameliorates methotrexate-induced hepatotoxicity in children and adolescents with acute lymphoblastic leukemia: a randomized placebo-controlled study, Nutrition 32 (1) (2016) 41–47.
[6] A.d.B. Tiphaine, L.L. Hjalgrim, J. Nersting, J. Breitkreutz, B. Nelken, M. Schrappe, M. Stanulla, C. Thomas, Y. Bertrand, G. Leverger, A. Baruchel, K. Schmiegelow, E. Jacqz-Aigrain, Evaluation of a pediatric liquid formulation to improve 6-mercaptopurine therapy in children, Eur. J. Pharm. Sci. 83 (2016) 1–7.
[7] A.F. Hawwa, J.S. Millership, P.S. Collier, K. Vandenbroeck, A. McCarthy, S. Dempsey, C. Cairns, J. Collins, C. Rodgers, J.C. McElnay, Pharmacogenomic studies of the anticancer and immunosuppressive thiopurines mercaptopurine and azathioprine, Br. J. Clin. Pharmacol. 66 (4) (2008) 517–528.
[8] X. Yuan, E. Gavriilaki, J.A. Thanassi, G. Yang, A.C. Baines, S.D. Podos, Y. Huang, M. Huang, R.A. Brodsky, Small-molecule factor D inhibitors selectively block the alternative pathway of complement in paroxysmal nocturnal hemoglobinuria and atypical hemolytic uremic syndrome, Haematologica 102 (2017) 466–475.
[9] P. Karran, N. Attard, Thiopurines in current medical practice: molecular mechanisms and contributions to therapy-related cancer, Nat. Rev. Cancer 8 (1) (2008) 24–36.
[10] K. Rowland, L. Lennard, J.S. Lilleyman, In vitro metabolism of 6-mercaptopurine by human liver cytosol, Xenobiotica 29 (6) (1999) 615–628.
[11] T. Dervieux, J.G. Blanco, E.Y. Krynetski, E.F. Vanin, M.F. Roussel, M.V. Relling, Differing contribution of thiopurine methyltransferase to mercaptopurine: thioguanine effects in human leukemic cells, Cancer Res. 61 (15) (2001) 5810–5816.
[12] J.A. Nelson, J.W. Carpenter, L.M. Rose, D.J. Adamson, Mechanisms of action of 6-thioguanine, 6-mercaptopurine, and 8-azaguanine, Cancer Res. 35 (10) (1975) 2872–2878.
[13] S. Haglund, J. Taipalensuu, C. Peterson, S. Almer, IMPDH activity in thiopurine-treated patients with inflammatory bowel disease –relation to TPMT activity and metabolite concentrations, Br. J. Clin. Pharmacol. 65 (1) (2008) 69–77.
[14] D.M. Tidd, A.R.P. Paterson, A biochemical mechanism for the delayed cytotoxic reaction of 6-mercaptopurine, Cancer Res. 34 (4) (1974) 738–746.
[15] L. Chouchana, A.A. Fernández-Ramos, F. Dumont, C. Marchetti, I. Ceballos-Picot, P. Beaune, D. Gurwitz, M.-A. Loriot, Molecular insight into thiopurine resistance: transcriptomic signature in lymphoblastoid cell lines, Genome Med. 7 (1) (2015) 37.
[16] T. Dervieux, T.L. Brenner, Y.Y. Hon, Y. Zhou, M.L. Hancock, J.T. Sandlund, G.K. Rivera, R.C. Ribeiro, J.M. Boyett, C.-H. Pui, M.V. Relling, W.E. Evans, De novo purine synthesis inhibition and antileukemic effects of mercaptopurine alone or in combination with methotrexate in vivo, Blood 100 (4) (2002) 1240–1247.
[17] J.M. Carethers, M.T. Hawn, D.P. Chauhan, M.C. Luce, G. Marra, M. Koi, C.R. Boland, Competency in mismatch repair prohibits clonal expansion of cancer cells treated with N-methyl-N'-nitro-N-nitrosoguanidine, J. Clin. Invest. 98 (1) (1996) 199–206.
[18] P. Pacher, A. Nivorozhkin, C. Szabó, Therapeutic effects of xanthine oxidase inhibitors: renaissance half a century after the discovery of allopurinol, Pharmacol. Rev. 58 (1) (2006) 87–114.
[19] M. Einhorn, I. Davidsohn, Hepatotoxicity of mercaptopurine, JAMA 188 (9) (1964) 802–806.
[20] S.P. Roche, R. Kobos, Jaundice in the adult patient, Am. Fam. Physician 69 (2) (2004) 299–308.
[21] G. Ma, J. Lin, W. Cai, B. Tan, X. Xiang, Y. Zhang, P. Zhang, Simultaneous determination of bilirubin and its glucuronides in liver microsomes and recombinant UGT1A1 enzyme incubation systems by HPLC method and its application to bilirubin glucuronidation studies, J. Pharm. Biomed. Anal. 92 (2014) 149–159.
[22] D. Zhang, T.J. Chando, D.W. Everett, C.J. Patten, S.S. Dehal, W.G. Humphreys, In vitro inhibition of UDP glucuronosyltransferase by atazanavir and other HIV protease inhibitors and the relationship of this property to in vivo bilirubin glucuronidation, Drug Metab. Dispos. 33 (11) (2005) 1729–1739.
[23] J. Zhou, T.S. Tracy, R.P. Remmel, Correlation between bilirubin glucuronidation and estradiol-3-gluronidation in the presence of model UDP-glucuronosyltransferase 1A1 substrates/inhibitors, Drug Metab. Dispos. 39 (2) (2011) 322–329.
[24] M. Vögelin, L. Biedermann, P. Frei, S.R. Vavricka, S. Scharl, J. Zeitz, M.C. Sulz, M. Fried, G. Rogler, M. Scharl, The impact of azathioprine-associated lymphopenia on the onset of opportunistic infections in patients with inflammatory bowel disease, PLoS One 11 (5) (2016) e0155218.
[25] E.A. Hullah, P.A. Blaker, A.M. Marinaki, M.P. Escudier, J.D. Sanderson, A practical guide to the use of thiopurines in oral medicine, J. Oral Pathol. Med. 44 (10) (2015) 761–768.
[26] P.P. Siva, K.M. Murali, A. Deepak, S. Murali, S. Michael, M. Sandhya, A novel liquid chromatography tandem mass spectrometry method for the estimation of bilirubin glucuronides and its application to in vitro enzyme assays, Drug Metab. Lett. 10 (4) (2016) 264–269.
[27] N.R. Beattie, N.D. Keul, A.M. Sidlo, Z.A. Wood, Allostery and hysteresis are coupled in human UDP-glucose dehydrogenase, Biochemistry 56 (1) (2017) 202–211.
[28] M. Kakehi, Y. Ikenaka, S.M.M. Nakayama, Y.K. Kawai, K.P. Watanabe, H. Mizukawa, K. Nomiyama, S. Tanabe, M. Ishizuka, Uridine diphosphate-glucuronosyltransferase (UGT) xenobiotic metabolizing activity and genetic evolution in pinniped species, Toxicol. Sci. 147 (2) (2015) 360–369.
[29] Z. Kaleta, B.T. Makowski, T. Soós, R. Dembinski, Thionation using Fluorous Lawesson's reagent, Org. Lett. 8 (8) (2006) 1625–1628.
[30] H.C. Koppel, R.K. Robins, Potential purine antagonists. XIII. Synthesis of some 8-methylpurines1, J. Organ. Chem. 23 (10) (1958) 1457–1460.
[31] T.K. Tam, B. Chen, C. Lei, J. Liu, In situ regeneration of NADH via lipoamide dehydrogenase-catalyzed electron transfer reaction evidenced by spectroelectrochemistry, Bioelectrochem. (Amsterdam, Netherlands) 86 (2012) 92–96.